



Numerical investigation of the effects of the vertical component of ground motion on seismic behaviour of soil slopes

Firooze Moghaddam¹

1- Geotechnical Engineer, Campbellreith Ltd.

MSc Geotechnics and Seismology: Imperial College London

firooze@moghaddam@campbellreith.com

Abstract

This paper investigates the effect of vertical component of earthquakes on stability of slopes using FE analysis. The analyses are conducted with the Imperial College Finite Element Program (ICFEP), using the Mohr-Coulomb failure criterion, and the generalized-decay Hyperbolic model accounting for elastic nonlinearity in small strain range. The models consist of slopes of different geometry constructed on deep saturated cohesive granular bedrock. These slopes are subjected to monotonic, harmonic, and seismic excitations. The response of models to these excitations is presented in terms of accumulated deformations, and plastic strains. These results indicate that the inclusion of vertical component leads to an increase in plastic deformation. This is in particular marked for steep models where a complete slope failure develops as opposed to the comparatively gentle slopes with localized plastic zones. The analyses suggest that ignoring the vertical component of earthquakes in seismic stability analysis can result in underestimation of the induced deformations, and can lead to an unsafe design. This can be more significant in the case of steep slopes.

Keywords: Vertical Excitation, Slope Stability, Finite Element Analysis, Embankment.

1. INTRODUCTION

Vertical ground motions have traditionally been neglected in evaluating the stability of slopes, since the contribution of the vertical component of an earthquake to the horizontal motion would have been considered insignificant. Peak Ground Vertical acceleration (PGV) was considered to be predominantly lower than 2/3 of the corresponding horizontal acceleration as proposed by Newmark (1973) [1]. This conclusion may have resulted from the limited availability of earthquake records as the vertical motions decay with distance in a much faster pace than the horizontals. However, some strong vertical excitations recorded recently have raised the question that to what extent the vertical component can affect the behaviour of structures and site response. [2]

Table 1.1: Examples of strong ground motions with high ratio of vertical to horizontal peak accelerations [2]

Event	Station(Mw)	Hor1(g)	Hor2(g)	Ver(g)	V/H
Gazli, Uzbekistan 1976	Karakyr(6.8)	0.71	0.63	1.34	1.89
Imperial valley, USA 1979	El cenro array 6 (6.5)	0.41	0.44	1.66	3.77
Nahhani, Canada 1985	Site1(6.8)	0.98	1.10	2.09	1.90
Morgan hill, USA 1984	Gilroy array#7(6.2)	0.11	0.19	0.43	2.25
Loma-prieta, USA 1989	LGPC(6.9)	0.56	0.61	0.89	1.47
Northridge, USA 1994	Arleta fire station(6.7)	0.34	0.31	0.55	1.61
Kobe, Japan 1995	Port Island (6.9)	0.31	0.28	0.56	1.79
Chi Chi, Taiwan 1999	TCU 076 (6.3)	0.11	0.12	0.26	2.07



Investigations on the effect of vertical acceleration carried out by various researchers as stated by Ambraseys and Douglas, 2000, suggest that ‘the seismic design without the consideration of the vertical ground motion component may result in unquantifiable risk from the collapse, especially those constructed in the close proximity of the fault’. Seismic excitations have a dual effect on foundations, soil slopes and earth dams. During an earthquake, on one hand large amounts of inertial forces are mobilized, and on the other hand, a significant deterioration of strength may occur. The latter can be caused by two processes: i. Excessive pore water pressure built up during the cycles of seismic loading, which can lead to liquefaction. In this type of strength deterioration, the horizontal and vertical components are equally effective; ii. The loss of cohesion due to post peak deformations. In creating this situation, both vertical and horizontal play a similar role. This is more noticeable in steep natural slopes, whose stability under gravity loads primarily is dependent on the peak strength, and any shock with sufficient intensity can impose large strains, and impair the cohesion. Even in the absence of horizontal component, a sufficient number of strong vertical acceleration pulses, can impair the cohesion and consequently result in a drop of strength from peak to residual, and lead to collapse [3].

The 2003 Bam earthquake with magnitude of 6.6 (Mw) struck the 2000-year-old Arg-e-Bam, and left the town in dust and ruin with the total fatalities of 26,271 people. Besides the structural damages, the near-source zone has also suffered from various geotechnical instabilities, such as; landslide, land subsidence and ground fissures, and understandably no liquefaction was observed due to the deep level of phreatic surface. The main characteristics of the instabilities were found to be the shallow slide, multiple block toppling, and Widespread deep tension cracks [4]. The reason for the demolition was found to be the vertical directivity effect led by the strong vertical component of the earthquake, 0.98g PGV [5]. However, no clear causative link has been suggested between the directivity effect and the widespread damage observed.

Ling et al. (2014) reappraised the reason of the 28m high Nigawa landslide occurred in Kobe earthquake, 1995, conducting a post analysis using pseudo-static method. The results suggested that strong vertical component of the Kobe earthquake had excited the landslide, in contrast to what previously been explained as a liquefaction effect. In addition, the shape of the slip surface was found to be deeper when incorporating larger contribution of the vertical component of the earthquake [6].

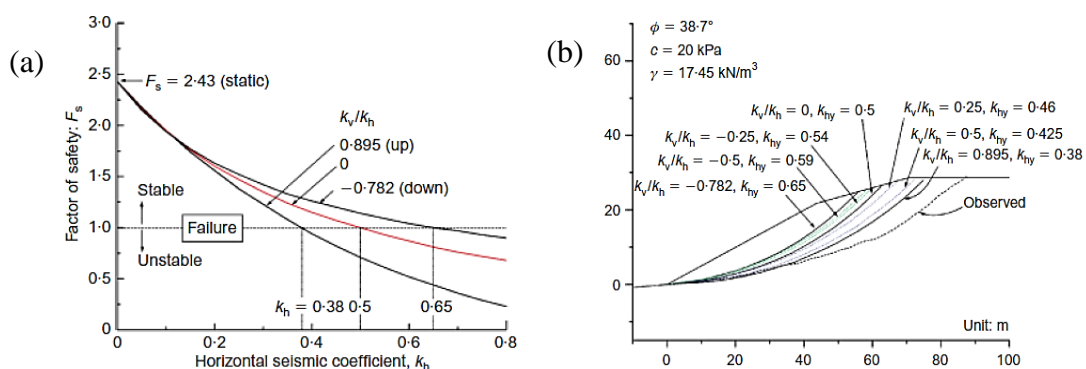


Figure 1.1: (a) Factor of safety versus horizontal seismic coefficient for variation in vertical seismic coefficient, (b): Analysed slip surfaces for different ratios of vertical to horizontal seismic coefficient [6]

Sarma and Scorer (2009) carried out numerous analyses on seismic stability of dry cohesionless slopes by Newmark Sliding Block method, incorporating the vertical component of two hundred earthquake records. The mean accumulated displacement in vertical excitation was found to be very low, and thus the conclusion was drawn in favour of the traditional design criteria as to neglect the effect of vertical ground motions in slope stability assessment. However, the author acknowledged that the number of outliers removed were large and need further investigations [7]. Simonelli and Stefano (2001) had also found similar results, using Newmark Sliding Block method to analyse the stability of dry, cohesionless slopes subjected to three major historical Italian earthquakes [8]. The latter authors employed similar methodology and assumptions for their analyses. However, in seismic stability investigations, the Newmark method suffers from serious limitations, as listed by Ingles (2006); 1) The sliding block is assumed to behave as a rigid-plastic body, 2) The block cannot have permanent deformations at accelerations below the critical acceleration, 3) Permanent plastic displacements are allowed for the body if the critical acceleration is exceeded, 4) The critical acceleration is



not related to strains and thus remains constant throughout the analysis, 5) Constant shear modulus is assumed for the sliding material, and is assumed to be constant at static and dynamic cases, and 6) The effects of dynamic pore pressure are neglected [9]. Therefore, the results cannot be considered as the most reliable source of information in this concept, and a need for more rigorous methods, such as; finite element, and boundary element approaches become more evident to provide more realistic model of soil behaviour and boundary conditions.

Gatmiri et al. (2007) performed a parametric study with boundary element approach for 2D elastodynamics in time-domain to investigate the effect of SV wave propagation on stability of slopes with respect to varying slope inclinations, and different excitation frequencies. It was found that: 1) steeper slopes accommodate larger displacements at the crest, and attenuation at the toe, 2) increase in the slope angle, generally amplify the response in both horizontal and vertical directions; however, for vertical incident shear waves, this is more pronounced in the vertical response. Also it was revealed that the ‘ η ’ parameter, defined as ratio of the slope height to the incident wave frequency, i.e. $\eta=H/\lambda$. plays an important role in this significance [10].

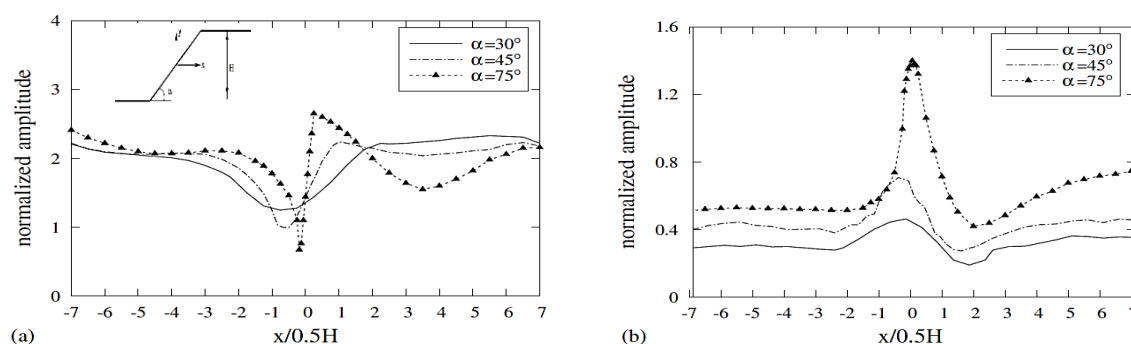


Figure 1.2: Slope response with variation in slope angle for $\eta=0.25$, where x is the distance from the mid-height point on the slope, and H is the slope height; a) horizontal displacement, and b) vertical displacement.

Zhang et al (2015) investigated the stability of near-fault large scale landslides, the Donghekou Landslide, induced by Wenchuan earthquake in 2008 ($M_s=8$). They employed a finite difference approach, and took into account the horizontal and vertical components. The results indicated that the incorporation of vertical component has a significant effect on the tension failure of blocks, as well as the sliding displacement. However, the influence on stability factor of safety was reported as insignificant [11]. Shinoda et al. (2013) performed a series of shaking table test on large-scale reinforced slope models. He also investigated the effects of vertical component on the stability of soil slopes, and drew similar conclusions [12].

2. NUMERICAL MODEL DESCRIPTION

It is well-known that the stability of slopes subjected to horizontal component decreases as the inclination angle increases. However, the effect of the effect of vertical seismic components on the stability of steep slopes has not been investigated extensively. In the present study, the model embankment with 3 inclination angles; 28°, 38°, and 48° were considered, while the height remained constant.

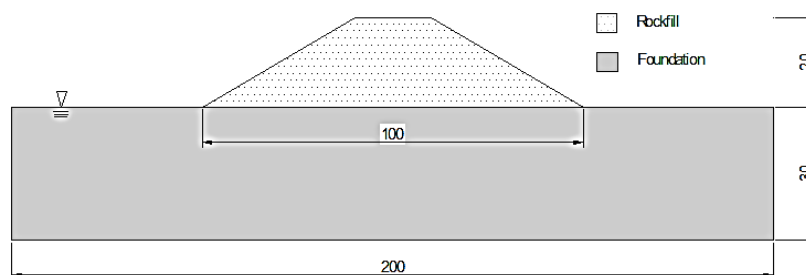


Figure 2.1: Typical geometry of the models



The response of FE analysis can be affected by the size of model discretization. Selection of coarse-sized meshes can filter the high-frequency components of dynamic excitations, since widely-spaced nodal points cannot model excitations with short wave length [13]. Therefore, in order to overcome this problem, as a rule of thumb, the maximum dimension of mesh size for 4-noded element should be limited to one-tenth to one-eighth of the shortest wavelength of all the material considered in the analysis [14]. Later in 1996, Bathe suggested that for 8-noded elements this criterion can be reduced to half (i.e. $\Delta l \leq \lambda/4 - \lambda/5$) [15]. Therefore, assuming 40Hz as the maximum frequency for vertical waves, and 8-noded quadrilateral elements, a minimum element size of 1.8m should be adapted. And also it was pointed out by Khosravi et al. (2013) that too fine-sized meshes should be avoided in finite element analysis of seismic slope stability as it may lead in underestimation of the results [16]. Therefore, in the first model (28°), a layer of transitional elements has been introduced in mid-height of the embankment to avoid having too fine meshes on the top of the crest, giving a total element number of 1395, whereas the other models with 1440 elements do not suffer from this problem since they have steeper side inclinations.

The materials used for the embankment modelled in the present study are based on properties of the main rock fill and foundation layer of well-documented Chinese dam, the Yele Dam. Soil parameters of the dam materials and dynamic properties of the rock fill were obtained from both laboratory and in-situ tests by He et al. (2006) [17], and Xiong (2009) [18] respectively, as cited by Han (2014) [19]. Figure 2.1 illustrates the general geometry of the models; the foundation is saturated cohesive granular rockfill, which is dried and processed to be used for the construction of the embankment.

Table 2.1: The material properties of the embankment [19]

Parameter	Cohesion	Angle of Shearing	Young's Modulus	Shear Modulus	Poisson's ratio	Density	S-wave Velocity	Permeability
Layer	c' (kPa)	ϕ' °	E (kPa)	G (kPa)	ν (g/cm ³)	ρ (g/cm ³)	Vs (m/s)	k (m/s)
Rock-fill embankment	10	50	7.34E+5	3.06E+5	0.2	2.3	364.7	1.00E-3
Foundation layer	80	38	3.53E+6	1.47E+6	0.2	2.3	800	1.00E-8

To enhance the prediction of soil deformations, a combination of three constitutive models were employed to better reproduce soil behaviour at different strain ranges, as follows:

1. An isotropic linear elastic model, namely following the Hook's law, is considered for the range of very small strains, i.e. zone 1 (~ less than 0.0003% as suggested by Vucetic (1994) [20], or less than 0.001% quoted by Ishihara(1996) [21]).
2. The general decay Hyperbolic model is used to simulate soil stiffness at small strain range (~between 0.0003% and 0.013%), and is coupled with the first model to predict the full-range pre-yield deformations.
3. The Mohr-Coulomb, an isotropic elastic perfectly plastic model is employed to introduce soil plasticity in the range of medium to large strain range.

To model the hysteresis behaviour of soil, the extended Masing rules [13] are implemented in the program. The classical Newton-Raphson (NR) method (i.e. Modified NR that is updated once) is introduced to the FE algorithm, as a robust solution strategy to solution to the true constitutive behaviour in shorter time [22]. Figure 2.2 provides a schematic summary of the constitutive models and stiffness correction schemes employed in the numerical analyses, as well as an example of the stress strain hysteresis behaviour at the toe when subjected to monotonic step loading in horizontal direction with 0.3g amplitude.

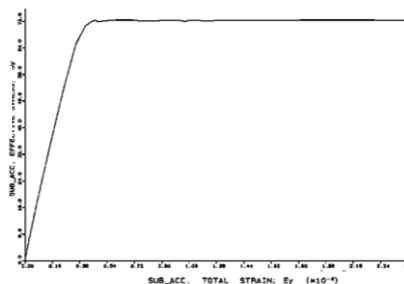
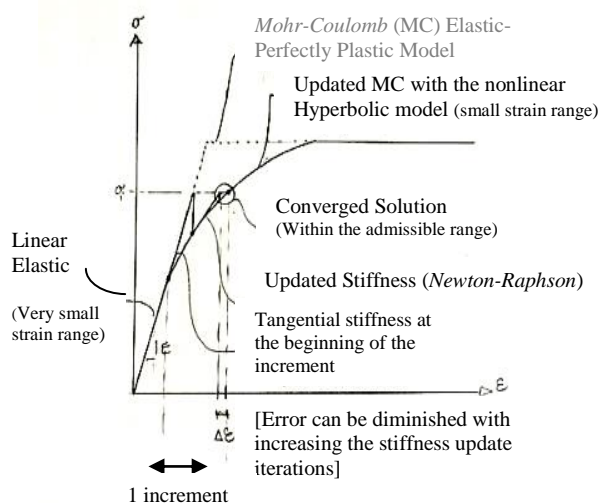


Figure 2.2: Summary of the constitutive models employed in the embankment model is schematically illustrated on the left. The right figure depicts the ICFEP output for the vertical hysteresis behaviour of element 1081, at the tow, when embankment is subjected to horizontal monotonic step loading of 0.5g magnitude for duration of 3 seconds.

The stability of the embankment models is studied assuming the plane strain condition. In static analyses, the history of slope layer-constructions is first simulated, and a period of 3.2 years is allowed for the consolidation stage, assuming standard fixity for the model boundary conditions. Then dynamic analyses are carried out by exerting the excitation acceleration on the foundation baseline. Tied degrees of freedom (TDOF) boundary condition is assumed for the lateral boundaries. TDOF originally introduced by Zienkiewicz et al. (1988) is essentially an elementary boundary condition in which the two nodes are tied together in order to deform identically [23]. These boundaries are acknowledged to satisfactory model the radiation damping of far-field response [24]. However, they must be placed far enough to sufficiently damp the energy of the propagating waves. It can be justified that by extending the lateral boundaries to a distance of full height of the model (Incl. foundation layer), no significant change in the accumulated displacement occurs under a sinusoidal vertical excitation of 4 Hz with an amplitude of 0.3g for 1 sec.

Table 2.1: Validation of the TDOF lateral boundary condition

Model No.	X	Model Geometry	Consolidation Settlement (cm) STATIC	Accumulated displacement under cyclic loadings (cm) DYNAMIC
1	0		4.31	4.85
2	1 H		4.45	5.01
3	2 H		4.46	5.02
4	5 H		4.46	5.02

3. RESULTS

Khosravi et al. (2013) categorised the failure criteria often considered in evaluation of FE results, as following; 1) Non-convergence of the solutions; this is not a generic rule, as it can also be the consequence of inappropriate configuration of the model in the FE program, such as not specifying stiffness update schemes (e.g. the Newton Raphson algorithm), or insufficient discretization of the times steps and element size, 2) Observation of a clearly defined failure surface along the side slopes, from the toe to the crest, 3) Rapid rise in displacements in the nodes on the side slopes; and 4) If a pre-defined equivalent shear or plastic strain magnitude is achieved along the potential failure surface; which is limited to the user judgement for the level



of strains defined and established prior to the analysis [16]. The 2nd and 3rd failure criteria are then adapted in this study. Failure of the slope models can be traced by inspecting the changes in the amplitude of the overall response. As shown in Figure 3.1, the vertical displacement at the crest varies almost linearly at the ground acceleration increases from 0.01g to 0.2g. As the intensity of excitation increases the response become slightly nonlinear resulting in relatively more deformation. As the ground acceleration exceeds 0.3g the response starts growing sharply with an exponential trend. This would clearly indicate the occurrence of a global failure as shown in Figure 4.5, where the development of a general slip surface is evident.

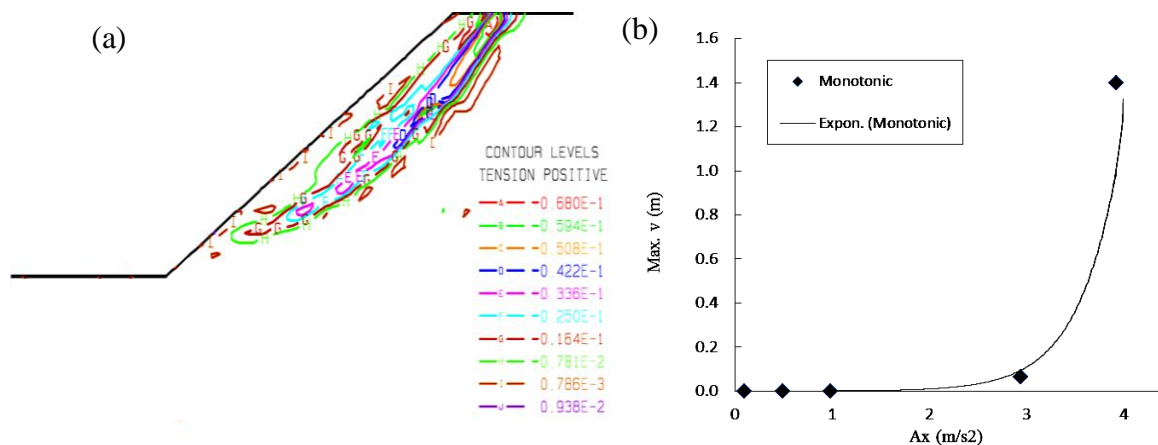


Figure 3.1: a) accumulated plastic vertical strain when the embankment is subjected to 0.4g monotonic loading, after 1 second of loading (i.e. Inc. 230), b) Maximum vertical displacement amplitude at the crest, induced by different magnitude of horizontal monotonic loadings (Acceleration).

Figure 3.2 demonstrates the influence of incorporating vertical loadings. As indicated before, when only horizontal monotonic step-acceleration is applied to the slope, failure occurs at 0.4g amplitude, and negligible deformation is induced at 0.2g. Then this is compared to the case that 0.2g horizontal acceleration is combined with 0.2g vertical acceleration of the same configuration. The results revealed a significant increase in the accumulated deformations in both directions.

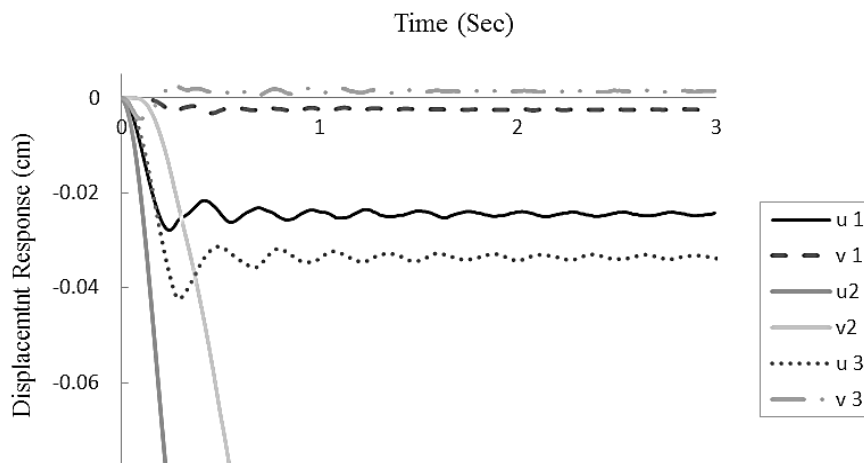


Figure 3.2: Sub-accumulated displacement time-history at the toe, when subjected to monotonic step loading: horizontal and vertical displacements are noted with u, and v respectively. Case 1: 0.2g amplitude in horizontal direction only, Case 2: 0.4g amplitude in horizontal direction only, Case 3: 0.2g amplitudes in both horizontal and vertical direction. (Note that the displacement axis is limited to 7cm in order to provide better resolution of the results). The reason for upward distribution of v3 is the upward vertical excitation disp.



The software ICFEP used to conduct the analyses was found remarkably capable of accounting for material and geometrical nonlinearities in soil media. Figure 3.3 demonstrates nonlinear hysteresis strain curves at Element 1181. It shows cycles of plastic deformations developed during harmonic excitations.

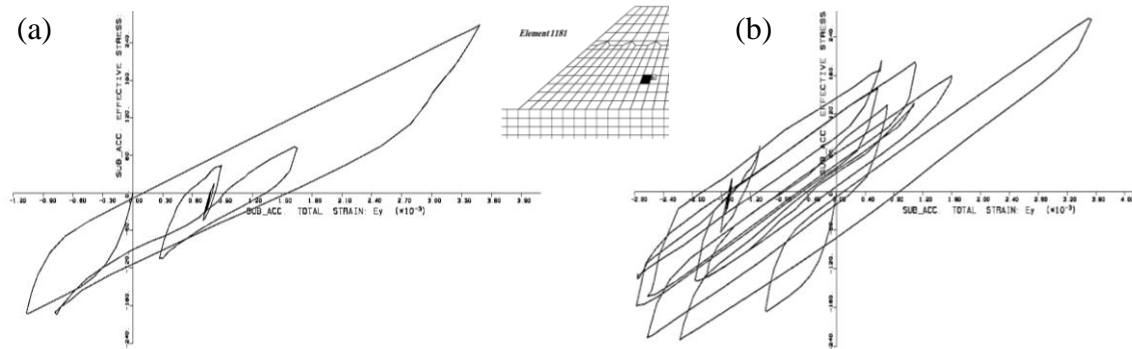


Figure 3.3: The plasticity progression by increase in the number of loading cycles: vertical stress-strain behaviour of element 1181; a) under a single sinusoidal pulse of amplitude 0.5g and period of 0.25sec, and b) subjected to 10 pulses of identical content.

The seismic record used for this study is the ground excitation recorded in Imperial Valley earthquake, 1979, at the ground surface of the ‘El Centro Array #6’ station which had the largest ratio of vertical to horizontal peak acceleration ($PGV= 1.5m/s^2$, and $PGA=0.35m/s^2$) ever recorded in the history. The most extreme response to this excitation is observed for the steepest embankment model (i.e. 48° slope). When the horizontal component of this seismic input motion is applied, only a localized highly plastic zone is observed at the toe, whilst a full slope failure is identified when the vertical component is combined with the latter. This can be clearly seen from the deformed shape of the slope, and the densely-spaced contours of large plastic strains in the following figures.

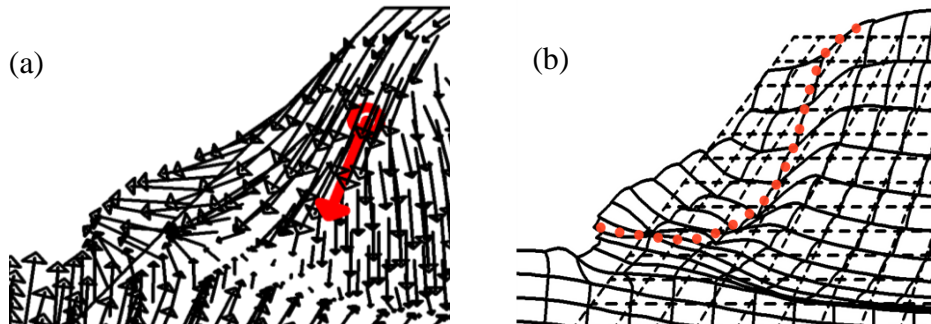


Figure 3.4: Zoomed in caption of the left inclination in figure 1.1 (Inc.: 331)

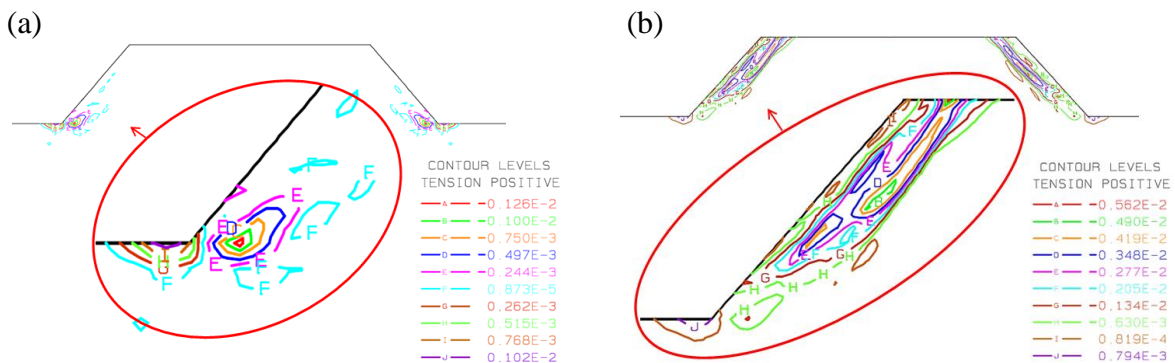


Figure 3.5: Contours of plastic vertical strains for 48° embankment, when subjected to:
a) only horizontal motion, b) both vertical and horizontal components of Imperial Valley record.



Figure 3.6 demonstrates the peak acceleration responses (PA) of the 28° slope model to the Imperial Valley record at the nodes along the centerline of the embankment. It can be seen that PA generally increases with height, although this is less pronounced in horizontal response as compared with the vertical. The PA response noticeably intensifies above the foundation level. A sharp rise in the peak acceleration in both horizontal and vertical directions is observed above the embankment base. This could partly be due to the abrupt reduction in the soil stiffness above the ground level as the embankment model is constructed of granular material significantly softer than the foundation. This is often referred to as the Impedance Effect. However, the Impedance alone may not be sufficient to justify this significant rise, and the geometry could play a part as the shape and size of the trapezoidal slope model is significantly different from the rectangular foundation model.

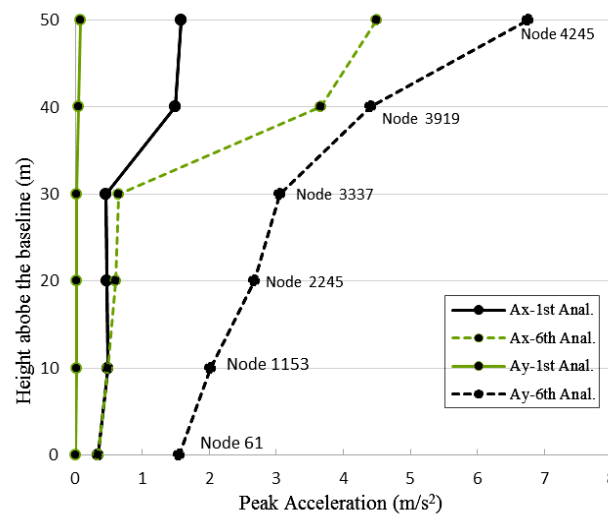


Figure 3.6: Comparison of the peak accelerations along the embankment centerline. [1st Analysis represents the case where the horizontal component of the Imperial Valley record is considered, and the vertical component is included in the 6th analysis]

4. CONCLUSIONS

1. The current state of practice traditionally neglects contribution of the vertical component of ground motions in assessment of slope stabilities. However, the results of nonlinear dynamic analyses of slopes subjected to the seismic excitations does not support this simplified view.
2. The present study indicates that neglecting the vertical motions can result in underestimating the induced deformations, and plastic strains reflected in the contours of the accumulated plastic strains.
3. In the present study, the model embankment with 3 inclination angles; 28°, 38°, and 48° were subjected to horizontal and vertical components of the seismic excitation. The results indicated that the inclination angle has a noticeable role on the stability of slopes, and the steep slopes are significantly more susceptible to instability when subjected to a combination of horizontal and vertical motions.
4. The results of analyses also demonstrated that the peak acceleration response, PA, generally increases with height, although this is less pronounced in horizontal response as compared with the vertical. PA response noticeably intensifies above the foundation level [26].



11. REFERENCES

1. Newmark, N.M., Blume, J.A. and Kapur, K.K. (1973). Seismic Design Spectra for Nuclear Power Plants, Journal of the Power Division, Proceedings of ASCE, Vol. 99, No. PO2, pp. 287–303.
2. Shrestha S.; (2009): Vertical ground motions and its effect on engineering structures: a state-of-the-art review. In: Proceeding of International Seminar on Hazard Management for Sustainable Development in Kathmandu, Nepal, 29-30 November 2009.
3. Ambraseys, N. and Douglas, J. (2000). Reappraisal of the effect of vertical ground motions on response. Report ESEE 00-4, Imperial College, London.
4. Amini Hosseini, K., Mahdaviifar, M. and Keshavarz, M. (2004) Geotechnical Instabilities Occurred During the Bam Earthquake of 26 December 2003, Journal of Seismology and Earthquake Engineering, Vol. 5 No. 4 and Vol. 6, No.1, Tehran
5. Zare, M, Hamzehloo, H. (2004), A Study of the strong ground motion of 26 December 2003 bam earthquake , Mw 6.5 , JSEE special Issue on Bam earthquake , vol 5&6, PP 33-56
6. Ling, H., Ling, H. I. & Kawabata, T. (2014) Revisiting Nigawa landslide of the 1995 Kobe earthquake. Geotechnique. 64 (5), 400-4.
7. Sarma, S.K., Scorer, M.R. (2009). The effect of vertical accelerations on seismic slope stability. International Conference on Performance Based Design in Earthquake Geotechnical Engineering, at Tokyo, Japan.
8. Simonelli, A.L., Stefano, PD. (2001). Effects of vertical seismic accelerations o slope displacement. International Conferences on Recent Advances in Geotechnical Earthquake Engineering and Soil Dynamics. Paper 23
9. Ingles, J., Darrozes, J. & Soula, J. (2006) Effects of the vertical component of ground shaking on earthquake-induced landslide displacements using generalized Newmark analysis. Engineering Geology. 86 (2-3), 134-147.
10. Gatmiri, B., Khoa-Van Nguyen & Dehghan, K. (2007) Seismic response of slopes subjected to incident SV wave by an improved boundary element approach. International Journal for Numerical and Analytical Methods in Geomechanics. 31 (10), 1183-95.
11. Zhang, Y., Zhang, J., Chen, G., Zheng, L. & Li, Y. (2015) Effects of vertical seismic force on initiation of the Daguangbao landslide induced by the 2008 Wenchuan earthquake. Soil Dynamics and Earthquake Engineering. 73, 91-102.
12. Shinoda M., Nakajima S., Nakamura H., Kawai T., Nakamura S. (2013) Shaking table test of large-scaled slope model subjected to horizontal and vertical seismic loading using E-Defense. Proceedings of the 18th International Conference on Soil Mechanics and Geotechnical Engineering, Paris Proceedings of the 18th International Conference on Soil Mechanics and Geotechnical Engineering, Paris.
13. Kramer, S. L. (1996). Geotechnical earthquake engineering. New Jersey: Prentice Hall.
14. Kuhlemeyer, R. L. and Lysmer, J. (1973). Finite element method accuracy for wave propagation problems. Journal of the Soil Mechanics and Foundation Division, ASCE, 99(SM5): 421-427.
15. Bathe, K. J. (1996). Finite element procedures in engineering analysis. New Jersey: Prentice Hall.
16. Khosravi, M., Leshchinsky, D., Meehan, C. L. & Khosravi, A. (2013) Stability analysis of seismically loaded slopes using finite element techniques. GeoCongress 2013: Stability and Performance of Slopes and Embankments III. 3-7 March 2013, Reston, VA, USA, American Society of Civil Engineers. pp.1310-19.
17. He, S., Hu, Y. and Liu, J. (2006). The asphalt concrete core rockfill dam in Yele hydraulic project (in Chinese). Hydraulic stations design, 22(2): 46-53.
18. Xiong, K. (2009). Seismic observations on Yele dam during the 2008 Wenchuan earthquake (in Chinese). Wuhan University. Government Report.
19. Han, B. (2014) Hydro-mechanical coupling in numerical analysis of geotechnical structures under multi-directional seismic loading. PhD. Department of Civil and Environmental Engineering of Imperial College London.
20. Vucetic, M. (1994). Cyclic threshold shear strains in soils. Journal of Geotechnical Engineering, 120(12): 2208-2228.
21. Ishihara, K. (1996) Soil Behaviour in Earthquake Geotechnics. 1st edition. , Clarendon Press.
22. Potts, D. M. and Zdravkovic, L. (1999). Finite element analysis in geotechnical engineering: Theory. London: Thomas Telford.



9th National Congress on Civil Engineering, 10-11 May 2016
Ferdowsi University of Mashhad, Mashhad, Iran



23. Zienkiewicz O.C., Bianic N. & Shen F.Q. (1988), "Earthquake input definition and the transmitting boundary condition", Conf: Advances in computational non-linear mechanics, Editor: St. Doltnis I., pp. 109-138.
24. Kontoe S, Zdravkovic L, Potts DM, Salandy NE et al., (2007), The use of absorbing boundaries in dynamic analyses of soil-structure interaction problems, Thessaloniki, Greece, Proceedings of the 4th International Conference on Earthquake Geotechnical Engineering
25. PEER website: (USGS) <http://pubs.usgs.gov/of/1982/1040/report.pdf> [accessed: July 2015]
26. Moghaddam, F. (2015) Numerical investigation of the effects of the vertical component of ground motion on seismic behaviour of soil slopes, MSc thesis, Department of Civil and Environmental Engineering of Imperial College London